Supporting information

Unlocking non-characteristic near-infrared emission of rare earth ions for photosynthetic bacteria cultivation and veins imaging applications

He Lin,[a] Shuangqiang Fang,*[a] Tianchun Lang,[b] Jiali Yu,[a] Haoliang Cheng,[a] Jiaqi Ou,[a] Zhijie Ye,[a] Renjie Xu,[a] Xiulan Shui,[a] Haolin Qu,[a] Le Wang *[a]

[a] College of Optical and Electronic Technology, China Jiliang University, Hangzhou 310018, China

[b] Chongqing Key Laboratory of Materials Surface & Interface Science, Research Institute for New Materials Technology, Chongqing University of Arts and Sciences, Chongqing 402160, China

Corresponding authors.
E-mail: fsq1025@163.com; calla@cjlu.edu.cn

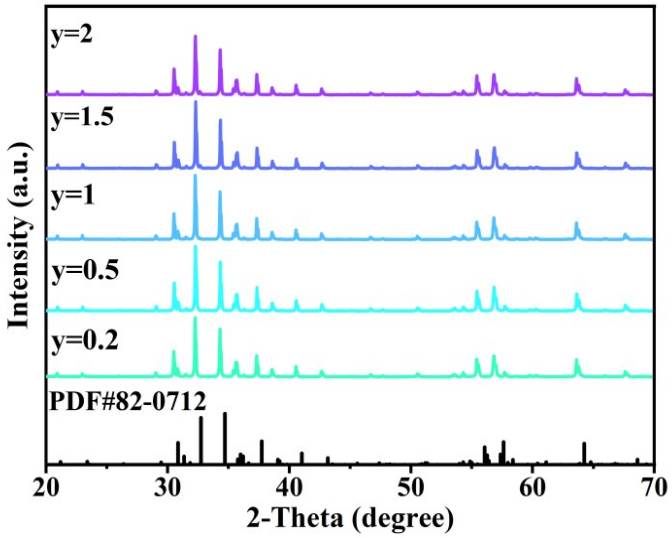

Figure S1. XRD patterns of $SrGa_{11.91-y}In_yO_{19}$:7%Cr^{3+},2%Tm^{3+}(y = 0.2 - 2)

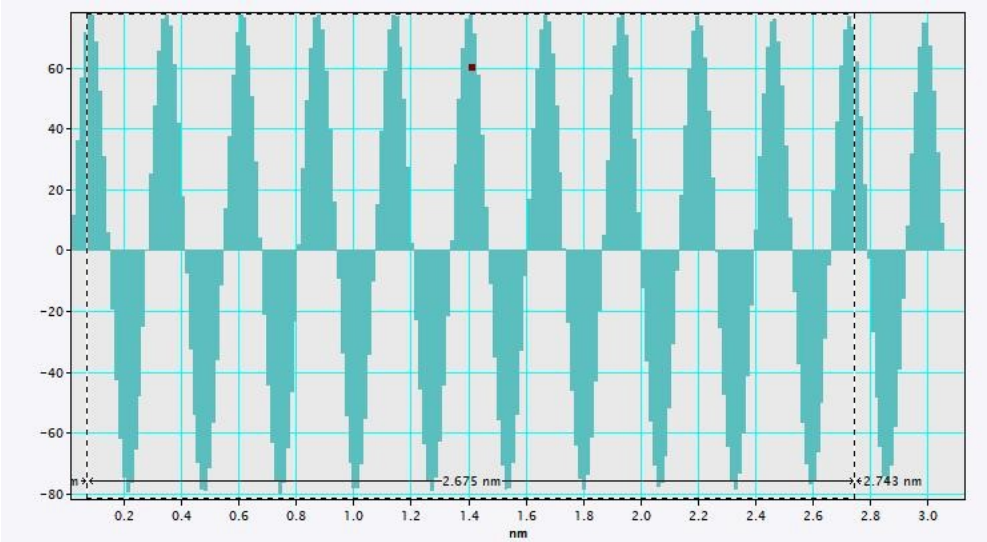

Figure S2. Lattice Stripes of $SrGa_{10.91}InO_{19}$:7%Cr^{3+},2%Tm^{3+}.

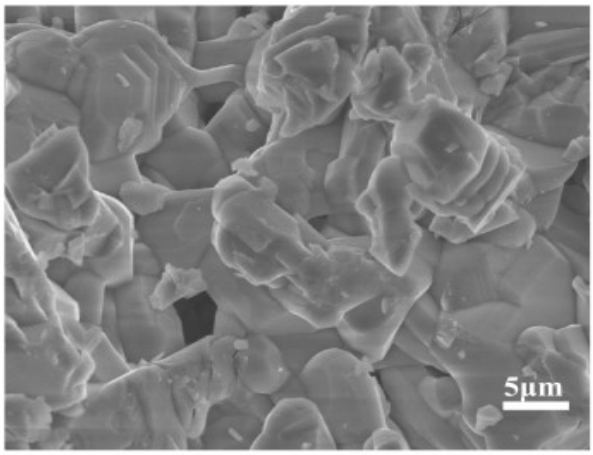

Figure S3. SEM image of $SrGa_{10.91}InO_{19}$:7%Cr^{3+},2%Tm^{3+}.

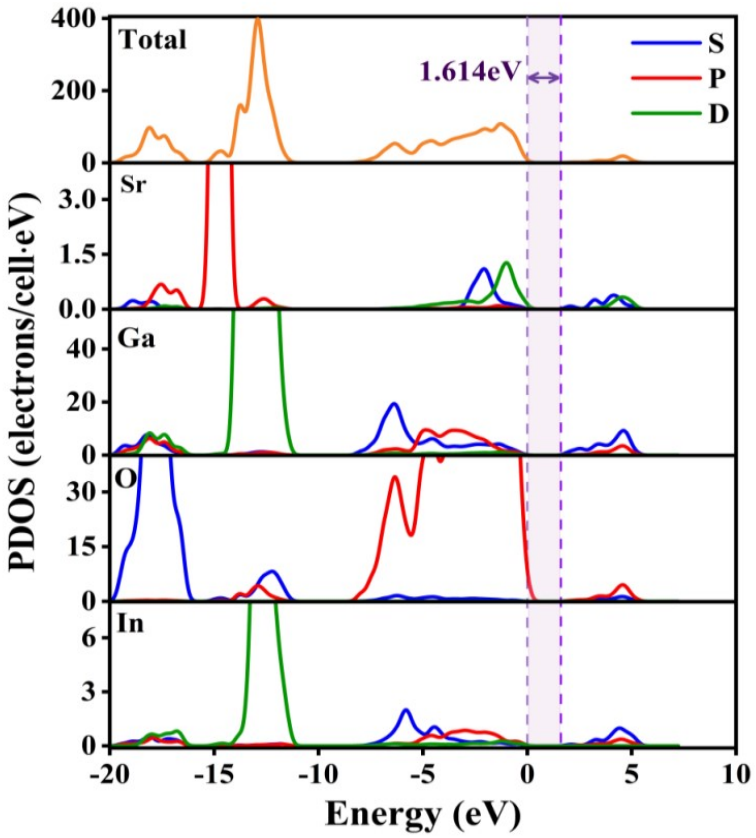

Figure S4. The total density of states(T-DOS), and partial density of states (P-DOS) of the $SrGa_{11}InO_{19}$.

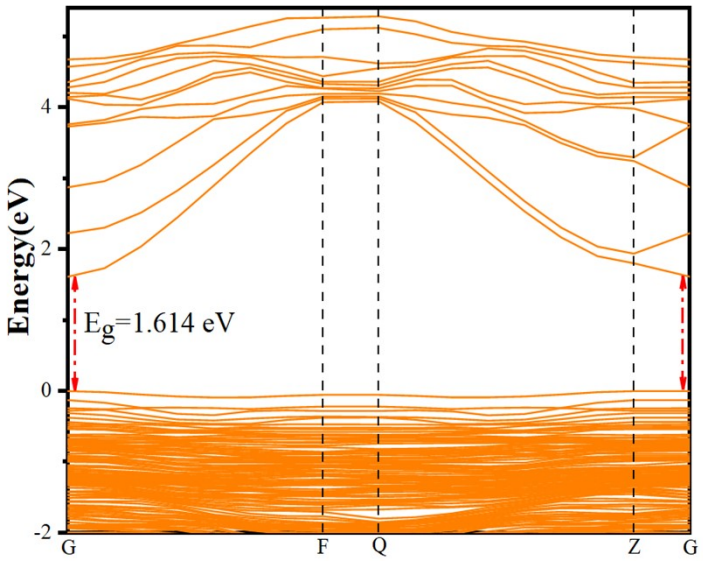

Figure S5. The band structure of $SrGa_{11}InO_{19}$

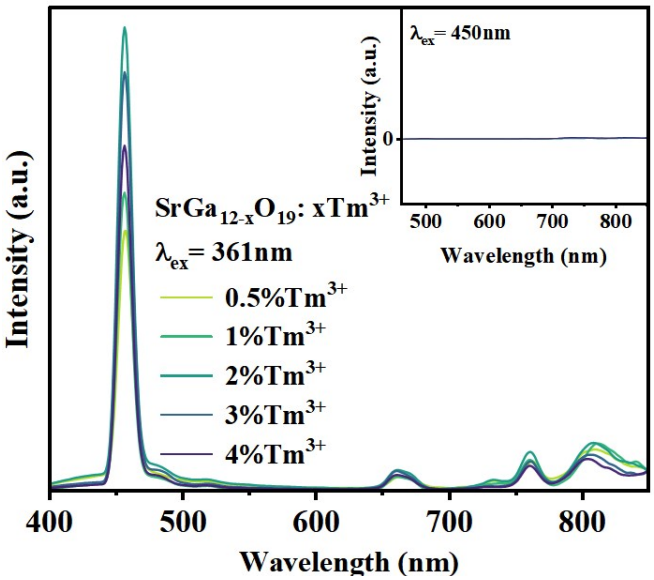

Figure S6. PL spectra of $SrGa_{12-x}O_{19}:xCr^{3+}$ (x = 0.5% - 4%), the inset shows the PL spectrum under 450 nm excitation.

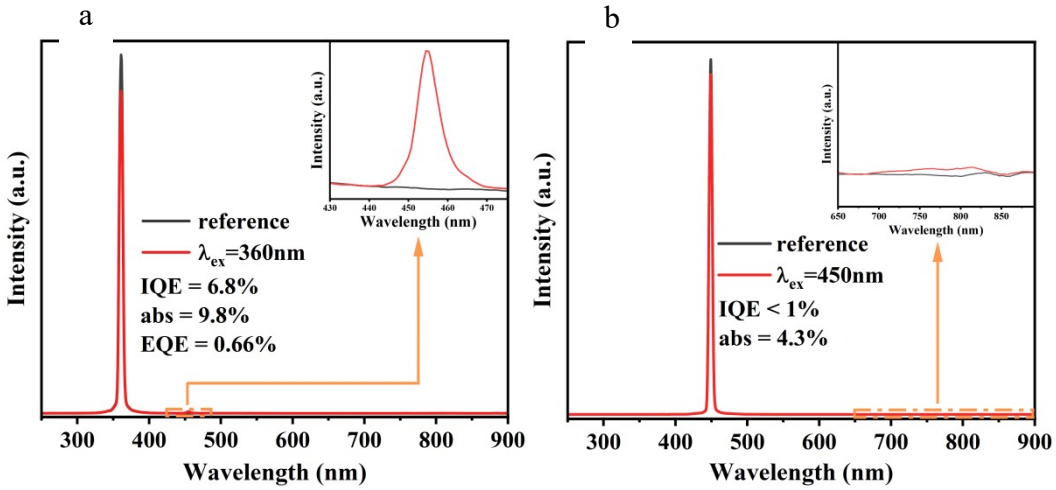

Figure S7. a、QE measurement of $SrGa_{11.98}O_{19}:2\%Tm^{3+}$ excited at 360 nm. **b**、QE measurement of $SrGa_{11.98}O_{19}:2\%Tm^{3+}$excited at 450 nm

IQE represents the ratio between emitted and absorbed photons, while EQE signifies the ratio between emitted photons and the total photons stimulated by the light source. Meanwhile, absorption efficiency (α_{Abs}) reflects the proportion of absorbed photons in the sample compared to the total photons stimulated by the light source. This connection between IQE, EQE, and α_{Abs} can be mathematically expressed as follows:[1]

$$IQE = \frac{\int E_{emS} - \int E_{emB}}{\int E_{exB} - \int E_{exS}} \times 100\% \quad (1)$$

$$EQE = \frac{\int E_{emS} - \int E_{emB}}{\int E_{exB}} \times 100\% \quad (2)$$

$$\alpha_{abs} = \frac{\alpha}{\delta} = \frac{\int E_{exB} - \int E_{exS}}{\int E_{exB}} \times 100\% \quad (3)$$

$$EQE = IQE \times \alpha_{abs} \quad (4)$$

where δ is the number of total photons excited by the light source and α is the number of photons absorbed by the sample. E_{exB} is the spectrum of the excitation light with $BaSO_4$ reference material in the sphere; E_{exS} is the spectrum of the excitation light with the sample in the sphere; E_{emB} is the spectrum of the emission light with the $BaSO_4$ in the sphere, and E_{emS} is the spectrum of the emission light with the sample in the sphere.

In the above-mentioned equations, δ represents the total number of photons stimulated by the light source, while α stands for the number of photons absorbed by the sample. Additionally, E_{exB} refers to the excitation light spectrum with $BaSO_4$ as the reference material within the sphere, E_{exS} represents the spectrum of the excitation light when the sample is placed inside the sphere, and E_{emB} signifies the spectrum of the emitted light with $BaSO_4$ located in the sphere. Finally, E_{emS} is the spectrum of the emitted light when the sample is placed inside the sphere.

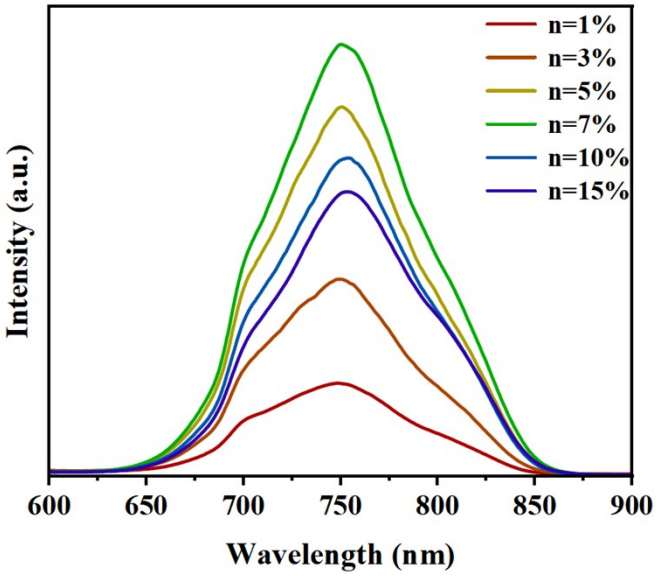

Figure S8. PL spectra of $SrGa_{12-n}O_{19}:nCr^{3+}$ (n = 1% - 15%).

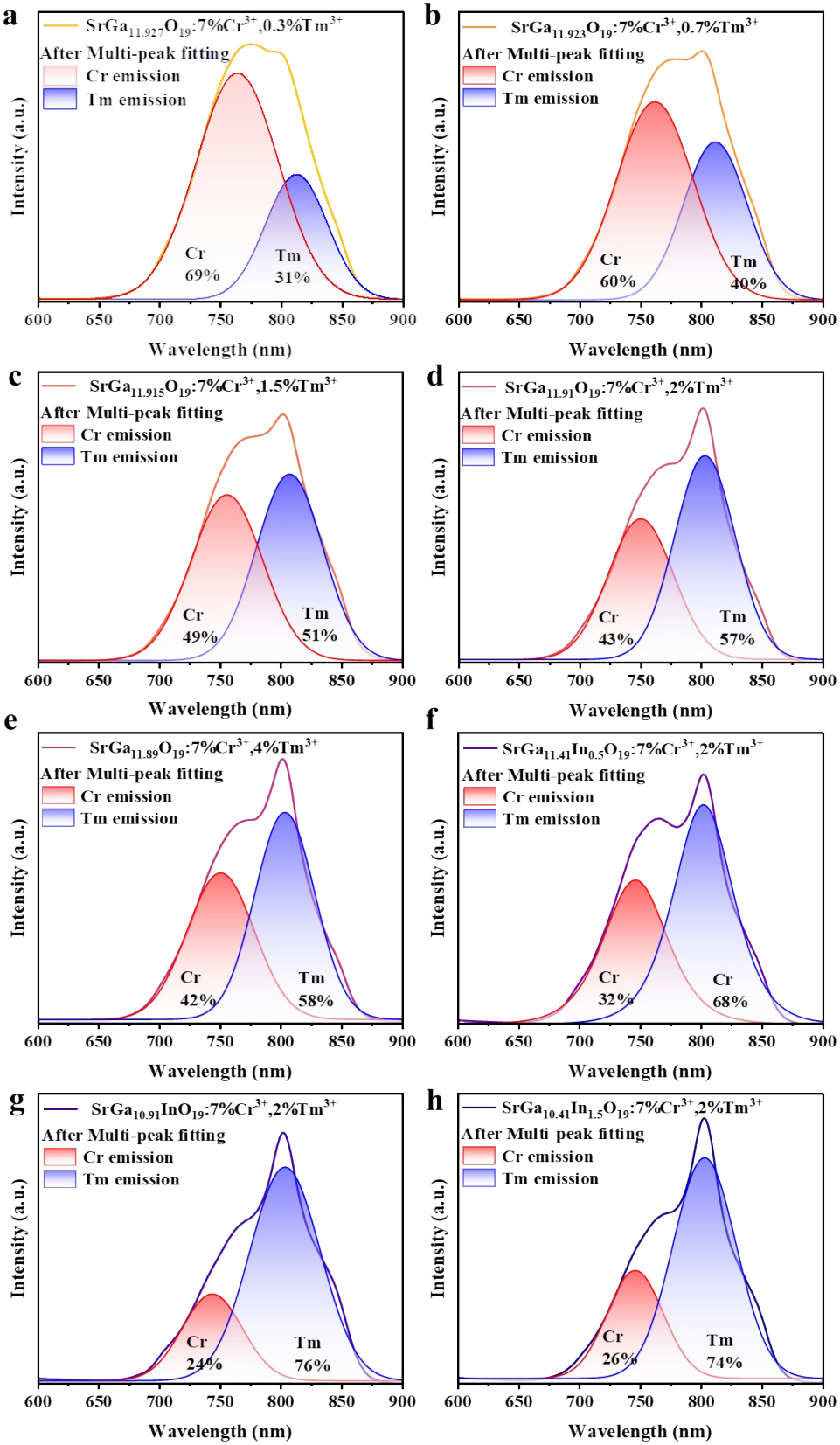

Figure S9. The ratio of Cr^{3+} and Tm^{3+} occupying the emission spectrum was calculated after multi-peak fitting of the emission spectra; a – e: $SrGa_{12-x}O_{19}$:7%Cr^{3+},x%Tm^{3+}, f - h: $SrGa_{11.91-y}In_yO_{19}$:7%Cr^{3+},2%Tm^{3+}

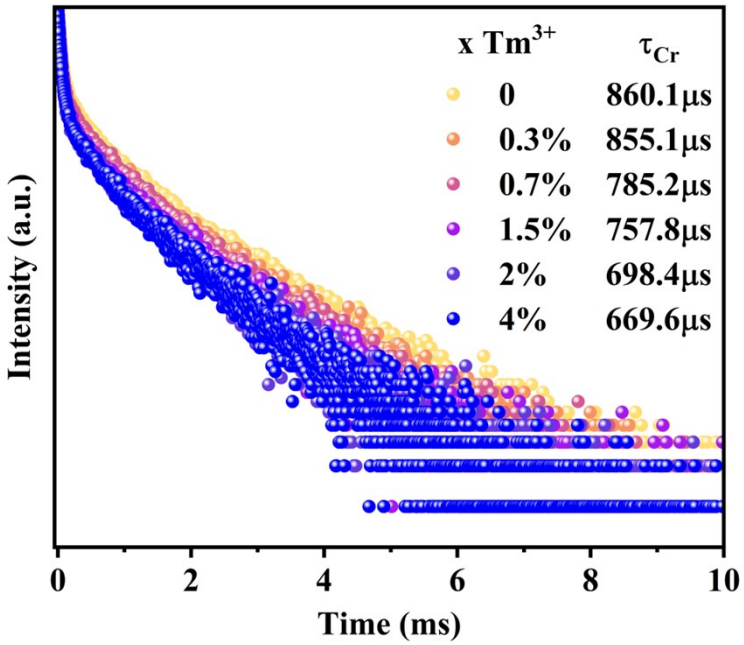

Figure S10. Decay curves of Cr^{3+} in $SrGa_{11.93-x}O_{19}$:7%Cr^{3+},xTm^{3+} (x = 0.3% - 4%) phosphors monitored at 740 nm with different Tm^{3+} concentration.

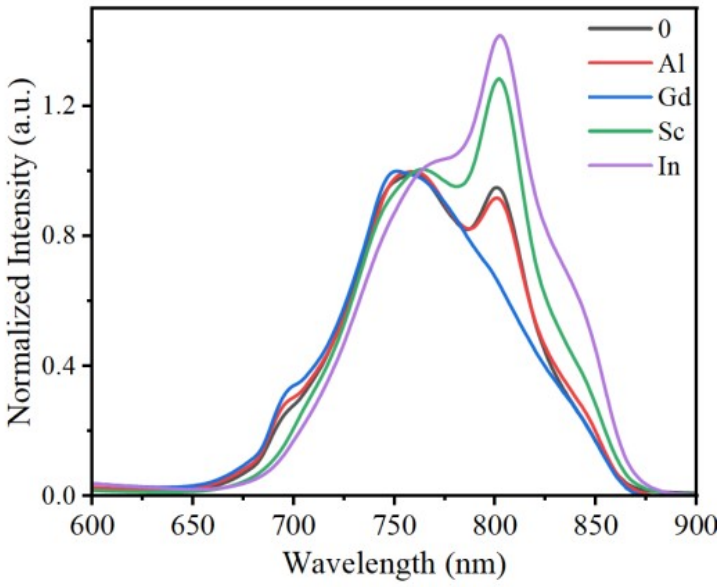

Figure S11. Normalized PL spectra of $SrGa_{10.91}XO_{19}$:7%Cr^{3+},2%Tm^{3+} (X = Al^{3+}, Gd^{3+}, Sc^{3+}, In^{3+}).

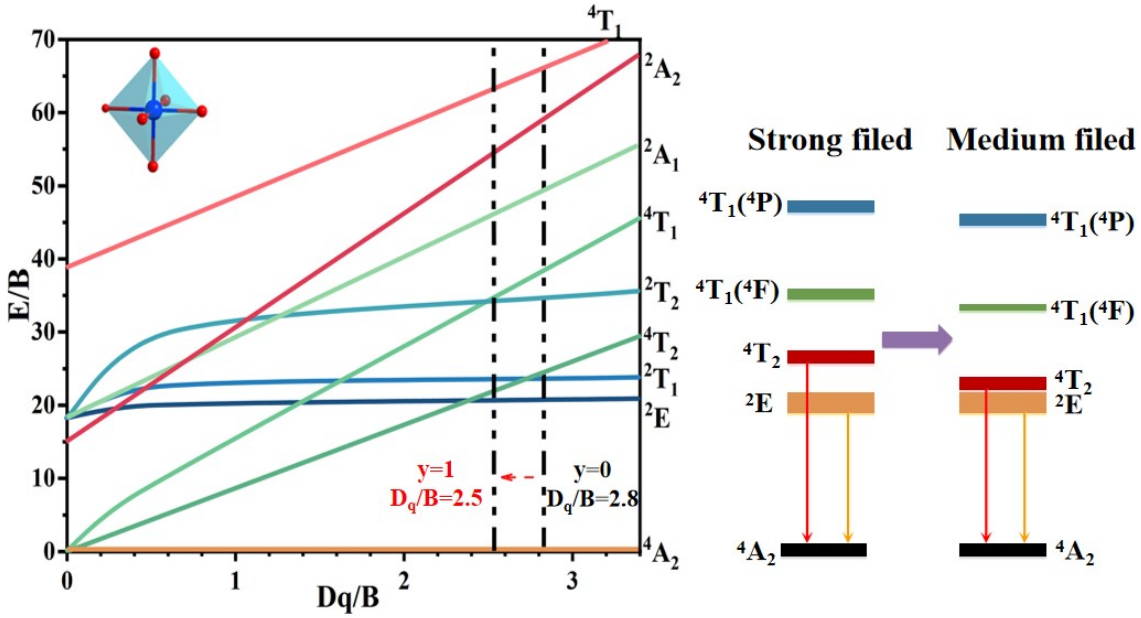

Figure S12. Tanabe-Sugano diagram of Cr^{3+} at an octahedron crystal environment dependence of emission spectra on In^{3+} concentration in $SrGa_{11.91-y}In_yO_{19}$:7%Cr^{3+},2%Tm^{3+}(y = 0, 1)

The crystal field intensity of $SrGa_{11.91-y}In_yO_{19}$:7%Cr^{3+},2%Tm^{3+} can be quantified employing the crystal field parameter D_q/B within the Tanabe-Sugano diagram.[2]

$$D_q = \frac{E(^4A_2 \rightarrow {}^4T_2)}{10} \quad (5)$$

$$m = \frac{E(^4A_2 \rightarrow {}^4T_1) - E(^4A_2 \rightarrow {}^4T_2)}{D_q} \quad (6)$$

$$D_q / B = \frac{15(m-8)}{m^2 - 10m} \quad (7)$$

Where D_q represents the crystal field parameters, and B corresponds to the Racah parameters. $E(^4A_2 \rightarrow {}^4T_1)$ and $E(^4A_2 \rightarrow {}^4T_2)$ denote the equilibrium positions of the excitation bands corresponding to the $^4T_1$ and $^4T_2$ energy levels, respectively. The computed values of D_q and B are approximately 1644 and 580 cm^{-1} for y=0 and around 1605 and 634 cm^{-1} for y=1. The resultant D_q/B ratios are 2.8 and 2.5, indicating a weakening of the crystal field.

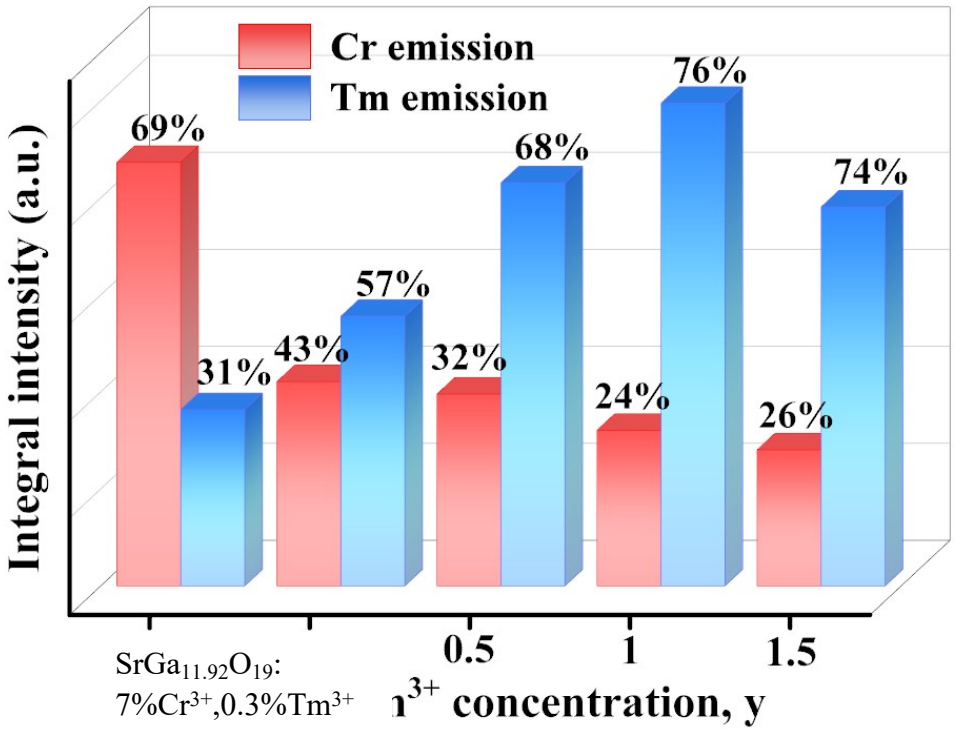

Figure S13. Ratio of the integrated intensity of Tm^{3+} emission to that of Cr^{3+} emission after In^{3+} introduction

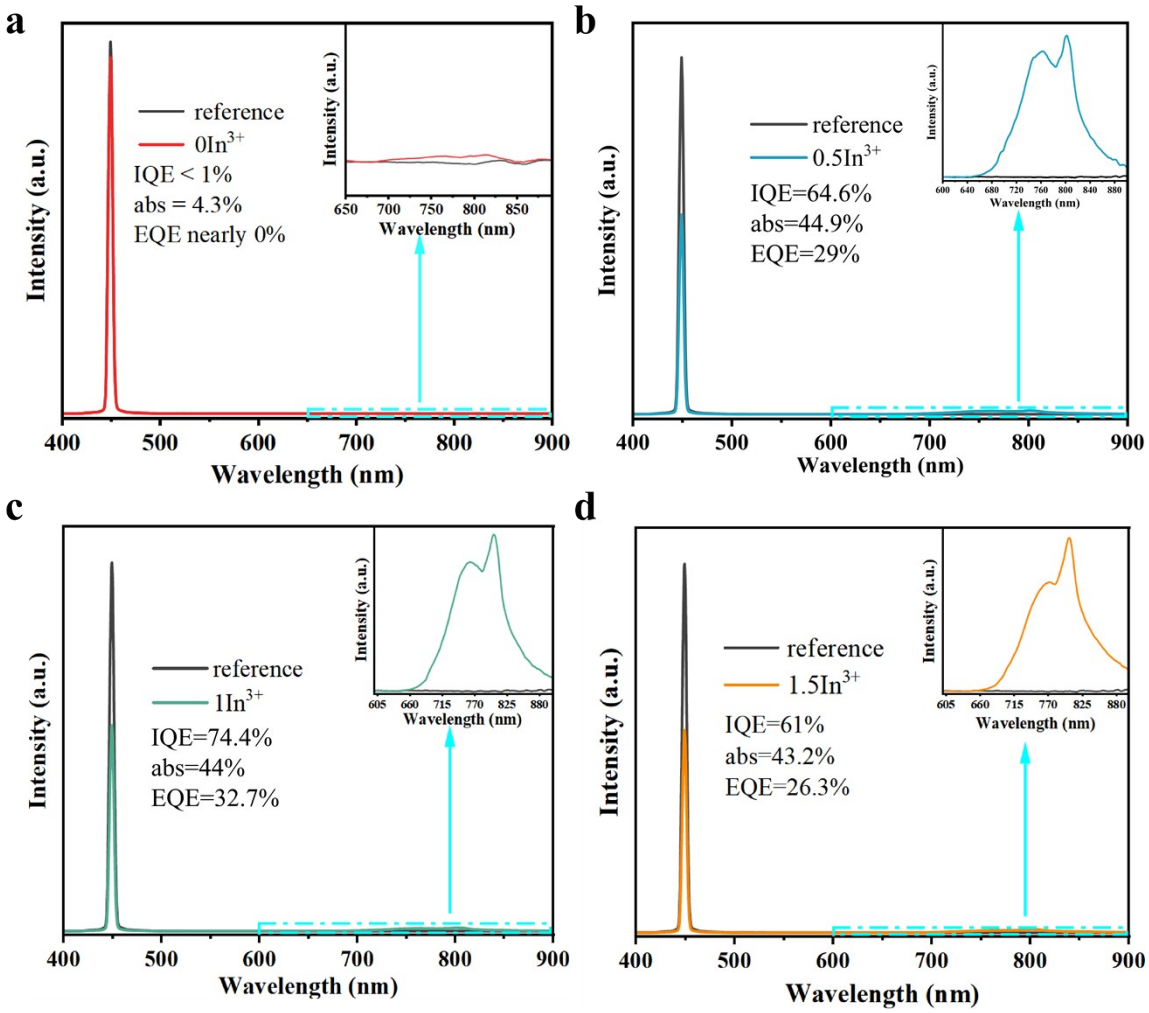

Figure S14. QE measurement of a) $SrGa_{11.98}O_{19}$:2%Tm^{3+}, b) $SrGa_{11.41}In_{0.5}O_{19}$:7%$Cr^{3+}$,2%$Tm^{3+}$, c) $SrGa_{10.91}InO_{19}$:7%Cr^{3+},2%Tm^{3+} and d) $SrGa_{10.41}In_{1.5}O_{19}$:7%$Cr^{3+}$,2%$Tm^{3+}$ excited at 450 nm.

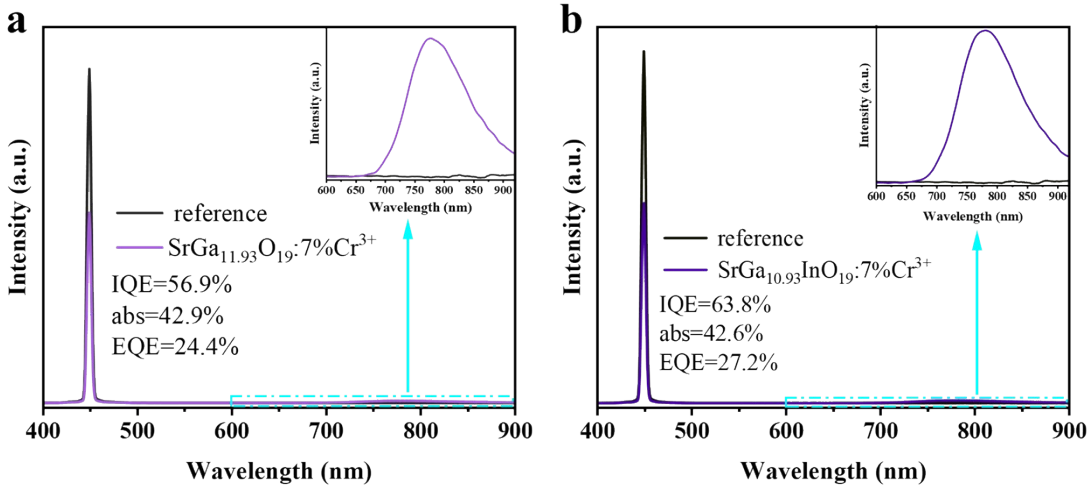

Figure S15. QE measurement of a) $SrGa_{11.93}O_{19}$:7%Cr^{3+}, b) $SrGa_{10.93}InO_{19}$:7%Cr^{3+} excited at 450 nm.

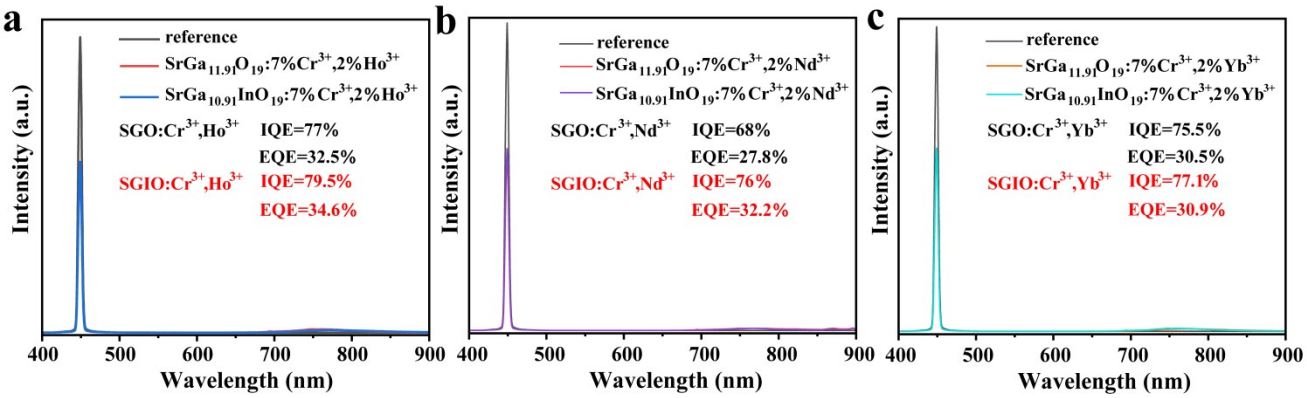

Figure S16. a) QE measurement of $SrGa_{11.91}O_{19}$:7%Cr^{3+},2%Ho^{3+} and $SrGa_{10.91}InO_{19}$: 7%Cr^{3+},2%Ho^{3+}excited at 450 nm. **b)** QE measurement of $SrGa_{11.91}O_{19}$:7%Cr^{3+},2%Nd^{3+} and $SrGa_{10.91}InO_{19}$:7%Cr^{3+},2%Nd^{3+}excited at 450 nm. **c)** QE measurement of $SrGa_{11.91}O_{19}$:7%Cr^{3+},2%Yb^{3+} and $SrGa_{10.91}InO_{19}$: 7%Cr^{3+},2%Yb^{3+}excited at 450 nm.

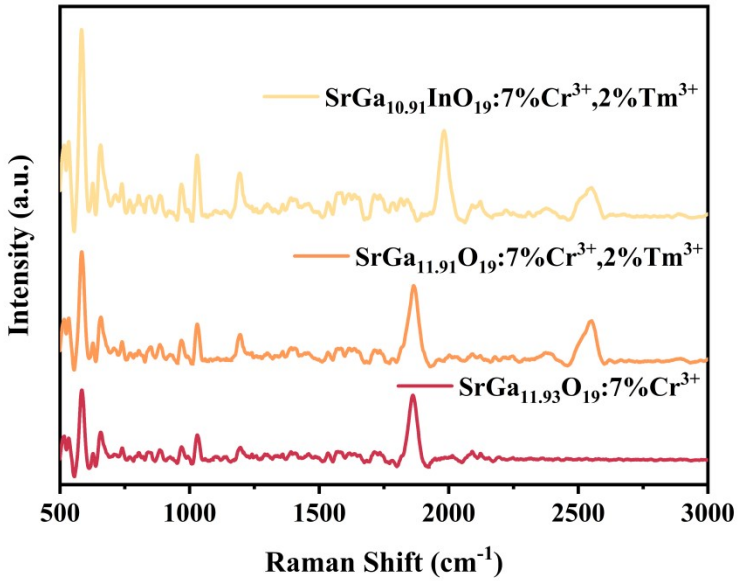

Figure S17. Raman spectrum of $SrGa_{11.93}O_{19}$:7%Cr^{3+}, $SrGa_{11.91}O_{19}$:7%Cr^{3+},2%Tm^{3+} and $SrGa_{10.91}InO_{19}$:7%Cr^{3+},2%Tm^{3+}

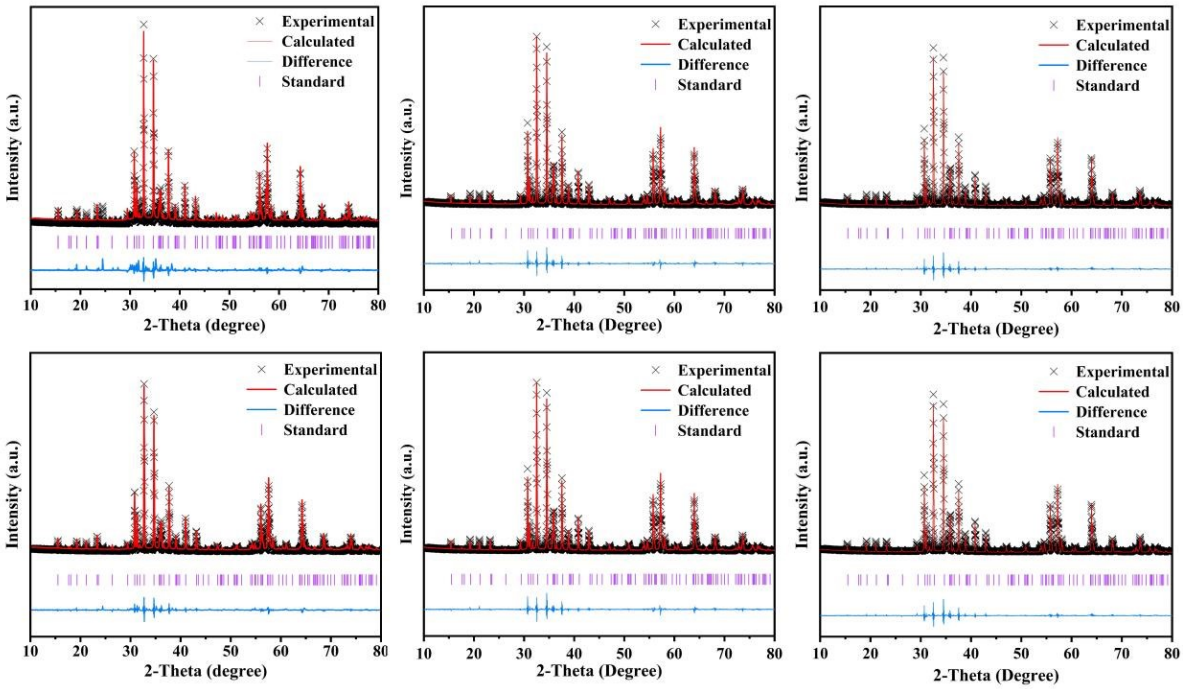

Figure S18. Rietveld refinements results of the $SrGa_{11.93-x}O_{19}$: 7%Cr^{3+},xTm^{3+} (x = 0.3% - 4%) and $SrGa_{11.91-y}In_yO_{19}$: 7%Cr^{3+},2%Tm^{3+} (y = 0.5 - 1.5)

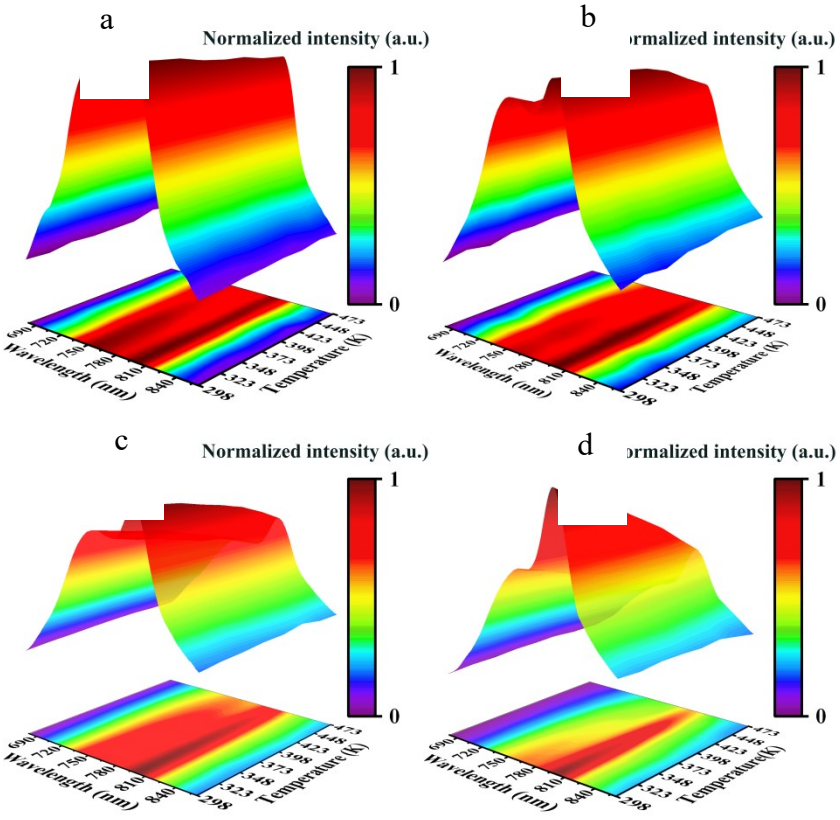

Figure S19. a - d、 The 3D temperature-dependent PL spectra of $SrGa_{11.91-y}In_yO_{19}$:7%Cr^{3+},2%Tm^{3+} phosphors

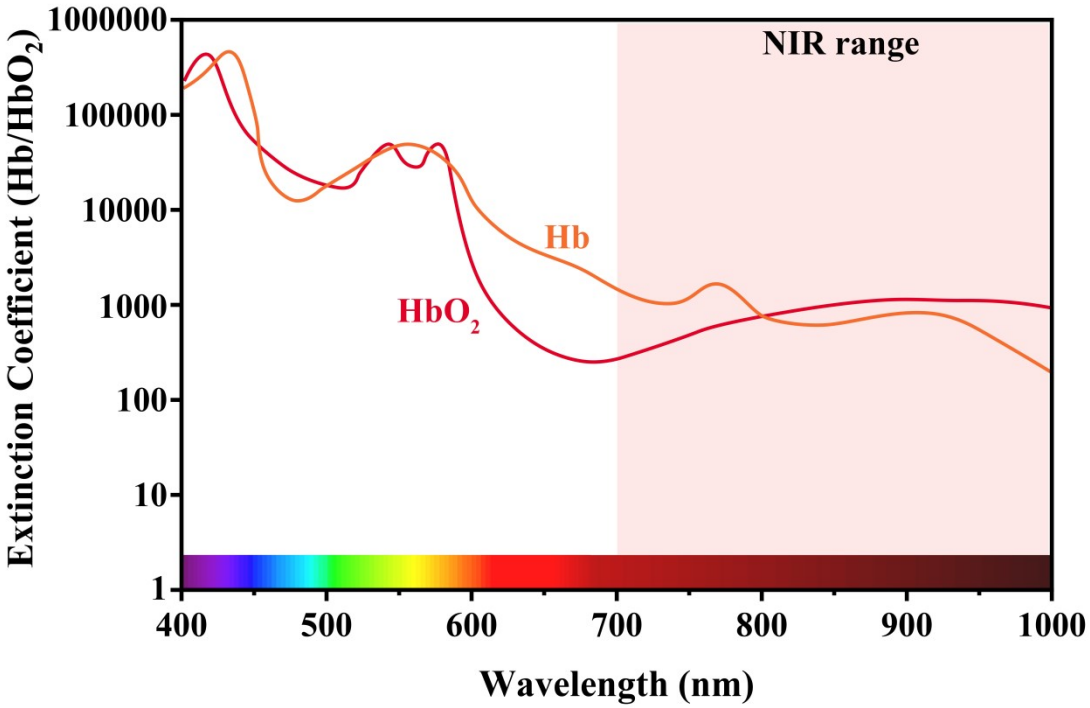

Figure S20. The absorption spectrum of human blood vessels.

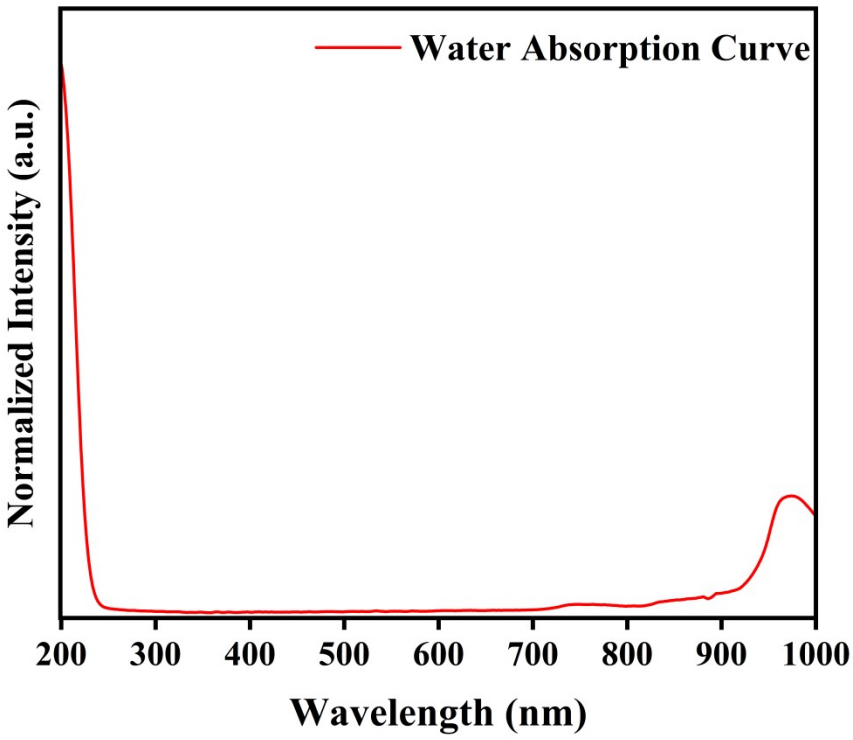

Figure S21. The absorption spectrum of water.

Table S1 Atom preferential site occupancies of In^{3+} and Tm^{3+} ions by utilizing Rietveld refinement for the representative $SrGa_{10.91}InO_{19}$:7%Cr^{3+},2%Tm^{3+} phosphor.

	Atom	x	y	z	Occ.
1	Sr	0.333	0.666	0.745	1
2	GaI	0.000	0.000	0.249	0.453
3	GaII	0.333	0.666	0.182	0.8
4	InI	0.000	0.000	0.215	0.028
5	InII	0.333	0.666	0.178	0.13
6	TmI	0.000	0.000	0.216	0.019
7	TmII	0.333	0.666	0.185	0.07

Table S2 Elemental content of Tm^{3+} and In^{3+} in $SrGa_{11.91}O_{19}$:7%Cr^{3+},2%Tm^{3+}, $SrGa_{11.41}In_{0.5}O_{19}$:7%$Cr^{3+}$,2%$Tm^{3+}$, and $SrGa_{10.91}InO_{19}$:7%Cr^{3+},2%Tm^{3+} samples by ICP-OES.

Test Element	Mole Ratio	Sample Weight (g)	Sample Content (mg/kg)	Elemental	Sample Elemental Content (%)
	2%	0.037	1836.94		0.184
Tm^{3+}	2%	0.036	2066.44		0.207
	2%	0.037	2564.86		0.256
	0	0.037	13.85		0.002
In^{3+}	0.5	0.036	39260.27		3.926
	1	0.037	80236.49		8.024

Table S3 Refined bond lengths for the $SrGa_{11.91}O_{19}$:7%Cr^{3+},2%Tm^{3+} and $SrGa_{10.91}InO_{19}$:7%Cr^{3+},2%Tm^{3+} samples

Bond length (Å)	$SrGa_{11.91}O_{19}$:7%Cr^{3+},2%Tm^{3+}	$SrGa_{10.91}InO_{19}$:7%Cr^{3+},2%Tm^{3+}
Ga-O1	1.85	1.98
Ga-O2	1.83	2.01
Ga-O3	1.91	1.84
Ga-O4	2.12	2.18
Ga-O5	1.73	1.75
Ga-O6	1.9	1.86
Tm1-Ga	2.69	2.63
Tm1-O3	1.75	1.56
Tm2-O3	2.01	2.08
Tm2-O5	2.13	2.33

Table S4 Refined bond angles for the $SrGa_{11.91}O_{19}$:7%Cr^{3+},2%Tm^{3+} and $SrGa_{10.91}InO_{19}$:7%Cr^{3+},2%Tm^{3+} samples

Band angle (°)	$SrGa_{11.91}O_{19}$:7%Cr^{3+},2%Tm^{3+}	$SrGa_{10.91}InO_{19}$:7%Cr^{3+},2%Tm^{3+}
Ga1-O1-O1	101	
Ga1-O8-O1	83.1	112.5
Ga2-O2-O2	96.7	118.9
Ga3-O4-O4	93.5	84.5
Ga4-O5-O5	119.8	119.9
Ga4-O7-O5	92.3	87.9
Ga5-O4-O4		120
Ga5-Tm2-O4		90.8
Ga6-O1-O1		106.6
Ga7-O3-O3	115.6	96.1
Tm1-O3-O3	86.7	85.5
Tm2-O7-Ga5		180

Tm2-O3-O3		73.2	
	89.1		
Tm2-O5-O5		112	
	109.7		
Tm2-O7-O4		106.8	

Table S5 Refined results of $SrGa_{11.93-x}O_{19}$: 7%Cr^{3+},xTm^{3+} (x = 0.3% - 4%) and $SrGa_{11.91-y}In_yO_{19}$: 7%Cr^{3+},2%Tm^{3+} (y = 0.5 - 1.5) phosphor

Samples		Volume (Å^3)	Tm-O_3,O_5 bond angle (°)	Tm-O bond length (ave Å)	Rwp, Rp , χ^2,(%)
$SrGa_{11.93-x}O_{19}$: 7%Cr^{3+},xTm^{3+}	0.3 %	662.985	95.3，105.7	1.937145	9.82, 8.83, 2.14
	0.7 %	662.747	96.5, 103.1	1.937329	9.48, 8.68, 2.07
	1.5 %	662.779	94.5, 103.5	1.937837	9.55, 8.78, 2.37
	4%	662.934	94.1, 102.9	1.937964	9.96, 8.87, 3.52
$SrGa_{11.91-y}In_yO_{19}$: 7%Cr^{3+},2%Tm^{3+}	0.5	672.833	91.3, 110.8	2.001681	7.29, 7.15, 2.67
	1.5	674.856	89.9,115	2.030385	8.38, 8.53, 3.56

Ethics statement

This study adheres to the principles outlined in the Declaration of Helsinki concerning medical research ethics. Prior to the commencement of the study, venous imaging participants were fully informed about the study's purpose, procedures, potential risks, and benefits. Informed consent was obtained from all participants, who agreed to participate in the study and to the publication of the study results. Throughout the study, all collected participant information was treated with strict confidentiality and used solely for the purposes of this research, ensuring the privacy and data security of the participants.

Reference

1 J. Qiao, S. Zhang, X. Zhou, W. Chen, R. Gautier and Z. Xia, *Adv. Mater.*, 2022, **34**, 2201887.

2 Y. Wang, Z. Wang, G. Wei, Y. Yang, S. He, J. Li, Y. Shi, R. Li, J. Zhang and P. Li, *Chem. Eng. J.*, 2022, **437**, 135346.